

1
2
3
4
5
6
7
8
9
10
11
12
13
14
15
16
17
18
19
20
21
22
23
24
25
26
27
28
29
30
31
32
33
34

Possible causes of arc development in the Apennines, central Italy

Andrea Billi

Dipartimento di Scienze Geologiche, Università “Roma Tre”, Rome, Italy

and

Mara Monica Tiberti

Istituto Nazionale di Geofisica e Vulcanologia, Rome, Italy

Running title: *Arc development in the Apennines*

Correspondence:

Andrea Billi

Dipartimento di Scienze Geologiche,
Università “Roma Tre”
Largo S. L. Murialdo, 1
00146, Roma, Italy
Tel: +39 0657338016
Fax: +39 0657338201
Email: billi@uniroma3.it

35 **ABSTRACT**

36 In central Italy, geometry, kinematics, and tectonic evolution of the late Neogene Umbrian Arc,
37 which is one of the main thrusts of the northern Apennines, have long been studied. Documented
38 evidence for orogenic curvature includes vertical-axis rotations along both limbs of the arc and a
39 positive orocline test along the entire arc. The curvature's cause is, however, still unexplained. In
40 this work, we focused our attention on the southern portion of the Umbrian Arc, the so-called
41 Olevano-Antrodoco thrust. We analyze, in particular, gravity and seismic reflection data and
42 consider available paleomagnetic, stratigraphic, structural, and topographic evidence from the
43 central Apennines to infer spatial extent, attitude, and surface effects of a mid-crustal anticlinorium
44 imaged in the CROP-11 deep seismic profile. The anticlinorium has horizontal dimensions of about
45 50 by 30 km and is located right beneath the Olevano-Antrodoco thrust. Stratigraphic, structural,
46 and topographic evidence suggests that the anticlinorium produced a surface uplift during its growth
47 in early Pliocene times. We propose an evolutionary model in which, during late Neogene time, the
48 Olevano-Antrodoco thrust developed in an out-of-sequence fashion and underwent about 16° of
49 clockwise rotation when the thrust ran into and was then raised and folded by the growing
50 anticlinorium (late Messinian-early Pliocene time). This new model suggests a causal link between
51 mid-crustal folding and surficial orogenic curvature that is consistent with several available data
52 sets from the northern-central Apennines; more evidence is, however, needed to fully test our
53 hypothesis. Additionally, due to the occurrence of mid-crustal basement-involved thrusts in other
54 orogens, this model may be a viable mechanism for arc formation elsewhere.

55

56 **KEYWORDS:** oroclines, Apennines, fold and thrust belts, gravity anomalies, and seismic
57 reflection profiles.

58

59 INTRODUCTION

60 Arcuate belts are among the most ubiquitous but also enigmatic and debated structures within
61 orogenic settings (e.g., Marshak, 2004; Sussman and Weil, 2004). In a recent classification of
62 curved orogens, Weil and Sussman (2004) recognize primary arcs, progressive arcs, and oroclines.
63 Primary arcs, which are non-rotational curves, adopt their curvature during the initial phase of
64 deformation and experience no appreciable tightening and vertical-axis rotations during subsequent
65 deformation. In contrast, both oroclines and progressive arcs are rotational curves (e.g., Weil,
66 2006). Progressive arcs either acquire their curvature progressively throughout their deformation
67 history (i.e., thrust rotations accommodate continuous along-strike variations in shortening;
68 Sussman et al., 2004) or acquire a portion of their curvature during a subsequent deformation phase.
69 Oroclines acquire their curvature in a two step process consisting first of the formation of a linear
70 orogen and subsequently of the bending of that orogen to form an arc.

71 Distinguishing between oroclines, progressive arcs, and primary arcs is relatively simple when
72 the appropriate methods of surface investigation can be used (e.g., paleomagnetic, structural, and
73 stratigraphic analyses to understand the temporal relationship between thrusting and vertical-axis
74 rotations; Weil and Sussman, 2004). In contrast, understanding the curvature's causes is usually
75 difficult, among other reasons, because of the paucity of subsurface data.

76 In this paper, we address the problem of the curvature's cause for the case of the southern
77 portion of the Umbrian Arc (i.e., the so-called Olevano-Antrodoco thrust) in the Apennine fold-
78 thrust belt, Italy (Fig. 1). This belt includes two main orogenic arcs, namely the northern and
79 southern arcs (Fig. 1). These arcs are different in size, shape, shortening, and involved rocks, and
80 include a set of major and minor curved thrusts (Royden et al., 1987; Ghisetti and Vezzani, 1997;
81 Macedo and Marshak, 1999). It is widely accepted that the development of the greater external arcs
82 (i.e., presently buried beneath the Adriatic and Ionian seas; Fig. 1) is mostly the result of non-
83 cylindrical rollback of a subducting segmented lithosphere (Royden et al., 1987; Faccenna et al.,

84 2004; Rosenbaum and Lister, 2004). In contrast, the origin of several curved thrusts within the
85 greater northern and southern arcs is still unexplained.

86 Paleomagnetic studies of the Umbrian Arc provide conflicting interpretations on the
87 development of mountain belt curvature, namely (1) oroclinal bending of an originally linear orogen
88 (Channel et al., 1978; Eldredge et al., 1985; Muttoni et al., 1998), and (2) an arc with fold axes
89 trends that have no relationship to vertical-axis rotations recorded by paleomagnetic declinations
90 (Hirt and Lowrie, 1988). Recent paleomagnetic data from the Umbrian Arc (Fig. 1C) conclusively
91 demonstrate secondary orogenic curvature (Speranza et al., 1997; Mattei et al., 1998). In particular,
92 evidence was provided for a positive orocline test along the entire Umbrian Arc, whose curvature
93 was acquired by simultaneous, and opposite-sense, vertical-axis rotations of the arc's limbs mostly
94 after Messinian time (Mattei et al., 1995, 1998; Speranza et al., 1997; Muttoni et al., 1998). The
95 cause for such rotations is, however, still unclear. In addition, the Olevano-Antrodoco thrust shows
96 an even more evident curvature. Most authors (Eldredge et al., 1985; Calamita and Deiana, 1988;
97 Ghisetti and Vezzani, 1997) have hypothesized that the main cause for orogenic curvature of the
98 southern limb of the Umbrian Arc is connected with a contrasting mechanical competence of the
99 involved rocks (i.e., Latium and Sabina carbonates; Fig. 1B). According to this model, stiff
100 carbonate rocks in the central Apennines (i.e., Latium platform carbonates) restrained the
101 advancement of the arc's southern limb, thus causing a displacement gradient along the northern
102 Apennine thrusts and their subsequent curvature.

103 The Umbrian Arc intersects with the southern arc thrusts in the central Apennines, where the
104 CROP-11 deep seismic profile highlighted the presence of a thick mid-crustal anticlinorium (Billi et
105 al., 2006). This structure is located beneath the Olevano-Antrodoco thrust, which is the southern
106 limb of the Umbrian Arc (Fig. 1C). Our hypothesis is that the anticlinorium and the associated
107 crustal thickening may have caused a significant surface uplift, possibly constituting an obstacle to
108 the migration of the Olevano-Antrodoco thrust. We used gravimetric and seismic reflection data to
109 determine attitude and spatial extent of the anticlinorium and its geometric relationship with the

110 Olevano-Antrodoco thrust. We then combined our results with available paleomagnetic,
111 stratigraphic, structural, and topographic evidence to understand the influence of the anticlinorium
112 on the development of the southern limb of the Umbrian Arc. Based on this evidence, we argue that
113 our hypothesis of a causal relationship between mid-crustal folding and orogenic curvature in the
114 central Apennines is viable; more evidence is, however, needed to fully test our hypothesis.
115 Additionally, due to the occurrence of mid-crustal basement-involved thrusts in other orogens, this
116 model may be a viable mechanism for arc formation elsewhere.

117

118

119 **GEOLOGICAL SETTING**

120 *Regional Setting*

121 Within the framework of Alpine-Himalayan orogenesis, the Apennine fold-thrust belt developed
122 mostly during Neogene time as a consequence of tectonic convergence between the European and
123 African (i.e., Nubia) plates (Fig. 1). The parallel migration of the trench and orogenic wedge toward
124 the east and southeast occurred concurrently with westward and northwestward subduction of
125 oceanic lithosphere beneath the European plate and with the progressive involvement of the
126 Adriatic (African affinity) continental margin with contractional deformation (Malinverno and
127 Ryan, 1986; Royden et al., 1987; Dewey et al., 1989; Faccenna et al., 2004; Rosenbaum and Lister,
128 2004).

129 The Apennines are characterized by major NW-striking thrust sheets generally dipping toward
130 the southwest with gentle angles and verging toward the northeast (Fig. 1). Thrust imbrication
131 occurred mostly in a forelandward piggyback sequence (Fig. 2) with some out-of-sequence or
132 backward thrusting episodes (e.g., Ghisetti and Vezzani, 1997; Cavinato and DeCelles, 1999;
133 Patacca et al., 2008). The thrusting style of the Apennine belt has been for years the subject of
134 contrasting interpretations including, in particular, thin-skinned and thick-skinned styles (e.g.,
135 Ghisetti et al., 1993; Mazzoli et al., 2000). Because of the paucity of subsurface data, in most

136 sectors of the Apennine chain, it is still unclear if thin-skinned or thick-skinned thrusting is the most
137 appropriate model for structural style (e.g., Mazzoli et al., 2008; Steckler et al., 2008).

138 Normal faults and associated extensional basins of Miocene-Pleistocene age are widespread in
139 the Tyrrhenian side of the Apennines and also in the axial sector of the fold-thrust belt (Fig. 1B)
140 (Malinverno and Ryan, 1986; Barchi et al., 1998; Jolivet et al., 1998; Cavinato et al., 2002).
141 Through time, the locus of extension has progressively migrated toward the east (Fig. 2), parallel
142 but west of the eastward-migrating locus of contractional deformation (Malinverno and Ryan, 1986;
143 Patacca et al., 1992). The lag time between the onset of thrusting and initial extension at any given
144 locality in the central Apennines is about 2-4 m.y. (Fig. 2) (Cavinato and DeCelles, 1999).

145 Seismic data across the Apennines show that the crust thickness increases from a minimum of
146 about 22 km in the Tyrrhenian side of the belt, to a maximum of almost 50 km in the axial sector
147 (Barchi et al., 1998; Cassinis et al., 2003; Billi et al., 2006; Mele et al., 2006; Di Luzio et al., 2008).

148

149 *Central Apennines*

150 Major thrust sheets in the central Apennines (i.e., Volsci, Simbruini, Marsica, Morrone, Gran
151 Sasso, and Maiella thrust sheets; Fig. 1C) are mostly NW-striking, NE-verging structures (Parotto
152 and Pratlun, 1975; Vezzani and Ghisetti, 1993). Dimensions of the exposed portion of these thrust
153 sheets are between about 40 and 120 km along-strike and about 20-30 km across-strike. Most of
154 these structures are thrust systems consisting of several imbricate major and minor thrusts. For
155 instance, the Marsica thrust system includes several thrusts, of which the westernmost Vallelonga
156 thrust is a NW-striking NE-verging structure located to the west of the Fucino basin (Fig. 1C). The
157 subsurface prolongation of this structure is considered in our analysis of the CROP-11 profile (Fig.
158 3) to infer the age of mid-crustal deformation.

159 Toward the west, the Olevano-Antrodoco thrust is the N-trending southern limb of the Umbrian
160 Arc (Fig. 1B). Geometries, kinematic indicators, and stratigraphic relationships along and over this
161 fault show its contractional nature and reverse displacements (Salvini and Vittori, 1982; Cosentino

162 and Parotto, 1992; Corrado, 1995; Ghisetti and Vezzani, 1997). In addition to reverse
163 displacements, however, some kinematic indicators on the Olevano-Antrodoco thrust zone and
164 stratigraphic evidence show that this structure accommodated younger right-lateral strike-slip
165 displacements during late Neogene time, possibly during early Pliocene time (Castellarin et al.,
166 1978; Salvini and Vittori, 1982).

167 The Olevano-Antrodoco thrust marks an important surface lithologic transition. In the
168 hangingwall, Mesozoic pelagian carbonates and marls are the dominant lithology (Sabina
169 transitional carbonates in Fig. 1B) with some exceptions such as the Rocca di Cave shelf (Accordi
170 and Carbone, 1986). In contrast, the footwall mostly consists of Mesozoic platform carbonates
171 (Latium platform carbonates in Fig. 1B; Parotto and Praturlon, 1975; Accordi and Carbone, 1986).
172 The thickness of the Sabina and Latium carbonates is about 3 and 5 km, respectively (Parotto and
173 Praturlon, 1975; Accordi and Carbone, 1986). The contrasting thickness and rigidity of the soft
174 marly rocks (Sabina carbonates) to the west of the Olevano-Antrodoco thrust, and hard platform
175 carbonates (Latium carbonates) to the east has been considered the main cause for the formation of
176 the Umbrian Arc (e.g., Calamita and Deiana, 1988; Ghisetti and Vezzani, 1997). It should be
177 considered, however, that the Sabina carbonates include, at the succession bottom, the thick and
178 rigid Calcare Massiccio Formation (i.e., Jurassic platform carbonates), which controls the
179 deformation pattern of the entire succession (Coward et al., 1999). From exploratory well data, it is
180 known that the Calcare Massiccio Formation is about 0.8 km thick (Anelli et al., 1994).

181

182 ***Thrust Timing and Vertical-Axis Rotations***

183 In the central Apennines, detailed stratigraphic analyses on sedimentary rocks and, specifically,
184 on syntectonic sedimentary bodies filling temporally- and spatially-successive foredeeps and thrust-
185 top basins (Patacca et al., 1992; Cipollari and Cosentino, 1995; Patacca and Scandone, 2001)
186 constrain the thrust evolution (e.g., Cavinato and DeCelles, 1999; Cosentino et al., 2003). The
187 cessation of thrusting in each locality is marked by the onset of continental sedimentation driven by

188 the post-orogenic extensional tectonics. Fig. 2 presents a synoptic diagram of results from previous
189 studies showing that the central Apennines mostly grew by in-sequence thrusting between late
190 Tortonian (Volschi thrust) and early Pliocene (Gran Sasso and Maiella thrusts) times. In places,
191 adjacent synchronous thrusting occurred (e.g., Marsica and Morrone thrusts). Out-of-sequence
192 thrusting is documented for the Gran Sasso and Olevano-Antrodoco thrusts (Cipollari et al., 1993;
193 Ghisetti and Vezzani, 1997; Satolli et al., 2005). In particular, during late Messinian-early Pliocene
194 time, the Olevano-Antrodoco thrust was emplaced over late Messinian, siliciclastic, foredeep
195 deposits (i.e., flysch) exposed to the north of the Simbruini thrust (Cipollari et al., 1993; Cipollari,
196 1995). The age of thrusting (Fig. 2) along with the truncation relationship with earlier adjacent
197 thrusts, and with temporally- and spatially-successive foredeeps and thrust-top basins (Fig. 1C),
198 indicates that the late Messinian-early Pliocene activity of the Olevano-Antrodoco thrust was out-
199 of-sequence (Cipollari and Cosentino, 1995; Mattei et al., 1995). Some authors infer also additional
200 activity of the Olevano-Antrodoco thrust during early-middle Messinian time (Cipollari and
201 Cosentino, 1992; Cipollari et al., 1993; Cavinato and DeCelles, 1999). In contrast, based on the age
202 of foredeep deposits presently exposed to the east and west of the Olevano-Antrodoco thrust, Mattei
203 et al. (1995) argue that the Olevano-Antrodoco thrust did not develop earlier than late Messinian
204 time.

205 In the southern sector of the Umbrian Arc, and in the adjacent areas (Fig. 1C), three main
206 paleomagnetic domains are recognized (Mattei et al., 1995, 1998): (1) the Sabina region (i.e., the
207 Olevano-Antrodoco thrust sheet), which rotated clockwise by about 16° (95% confidence half-
208 angle, $\alpha_{95} = 11.5^\circ$) after early-middle Miocene time (Mattei et al., 1995) with no significant
209 rotations since middle Pliocene time (Sagnotti et al., 1994); (2) the Roveto Valley, which rotated
210 counterclockwise by about 28° ($\alpha_{95} = 10.5^\circ$) during post-Messinian times; and (3) the Tuscan-
211 Latium (i.e., Tyrrhenian side of the Apennines) neautochthonous basins (Neogene-Quaternary),
212 which have been affected by non-rotational deformation (Sagnotti et al., 1994; Mattei et al., 1996).

213

214 **THE CROP-11 SEISMIC REFLECTION PROFILE**

215 The CROP-11 deep seismic reflection profile was planned and acquired across the central
216 Apennines (Fig. 1C) to image the crustal-scale tectonic architecture of the junction between the
217 northern (i.e., Umbrian Arc) and southern orogenic arcs (Parotto et al., 2003). Parameters of
218 acquisition and processing of the CROP-11 profile are provided in a previous paper (Billi et al.,
219 2006). Time-to-depth conversion of the CROP-11 seismic profile was not attempted because
220 detailed velocities of P-waves in the study area were not appropriately known at the time of data
221 processing (now available in Di Luzio et al., 2008 and Patacca et al., 2008 for the eastern portion of
222 the seismic line).

223 The central segment of the CROP-11 profile (Fig. 3) shows the core of the orogenic wedge,
224 where strong reflections occur between about 5 and 8-9 s two ways travel time (TWTT). These
225 reflections outline a wide and thick anticlinorium that is interpreted as being developed above a
226 middle-lower crust shear zone occurring between about 7 and 9 s TWTT with variable dip angles.
227 From seismic refraction data (Cassinis et al., 2003), it is inferred that the shear zone is as deep as
228 about 20-22 km (i.e., corresponding to about 9 s TWTT). The anticlinorium is characterized by two
229 hinge zones imaged by two sets of upward-convex reflections (Fig. 3B). The vertical component of
230 displacement on the basal shear zone, as estimated on the CROP-11 profile, is about 2 s TWTT
231 corresponding to about 4-5 km.

232 In the CROP-11 profile, the near-surface portion of the Olevano-Antrodoco thrust is imaged as
233 a low-angle, shallow structure dipping toward the west and resting above the crest and backlimb of
234 the mid-crustal anticlinorium (Figs. 3B and 3C). The geometric relationship between the Olevano-
235 Antrodoco thrust and the underlying anticlinorium are not straightforward in the seismic image. The
236 weak, ramp-flat geometry (consisting of near-horizontal flats and low-angle ramps) of the Olevano-
237 Antrodoco thrust seems only partially parallel to the geometry of the underlying anticlinorium. In
238 particular, the hinge between the crest and the backlimb of the anticlinorium is not coincident with
239 the hinge between the ramp and flat segments of the Olevano-Antrodoco thrust. Moreover, the

240 interlimb angle of the anticlinorium is smaller than the angle between the flat and ramp segments of
241 the Olevano-Antrodoco thrust. These geometric relationships suggest that the Olevano-Antrodoco
242 thrust postdates the anticlinorium; however, some parallelism between the anticlinorium crest and
243 the Olevano-Antrodoco thrust main flat may represent evidence that the Olevano-Antrodoco thrust
244 was affected by some folding connected with anticlinorium growth.

245 To the west of and beneath the Fucino basin, some shallow reflections (shallower than 2 s
246 TWTT) located to the east of the mid-crustal anticlinorium are parallel to its forelimb (Fig. 3B).
247 Such a geometric relationship suggests that these shallow reflections were involved in the
248 anticlinorium-related folding and, therefore, that the anticlinorium postdated the shallow thrust
249 sheets located immediately to the east. The location of the E-dipping shallow reflections suggests
250 that they represent the eastward subsurface prolongation of the Marsica thrust sheet (i.e., the
251 bedding panels forming the Vallelonga thrust sheet; Fig. 3B), whose age is late Messinian-very
252 early Pliocene (Figs. 1C and 2). The overall E-dipping attitude (i.e., by about 20°) of the exposed
253 portion of the Vallelonga thrust sheet (Servizio Geologico d'Italia, 1968; Vezzani and Ghisetti,
254 1993) supports the hypothesis of a linkage between the exposed Vallelonga thrust sheet and the E-
255 dipping shallow reflections imaged in Fig. 3(B) to the west of and beneath the Fucino basin (see
256 also Patacca et al., 2008).

257

258 **ANALYSIS OF GRAVITY DATA**

259 We analyzed the regional gravity data of the central Apennines (Fig. 4) to determine the gravity
260 signature of the mid-crustal anticlinorium (Fig. 3B) and to infer its areal (i.e., map-view) extent.
261 The gravity dataset was obtained through a stripping-off procedure (sensu Hammer, 1963), which
262 consisted of removing the effect of all geological bodies located in the upper crust from the
263 Bouguer anomaly data (Carrozzo et al., 1991; Fig. 4A). The stripping-off procedure applied to
264 obtain the map shown in Fig. 4(B) is thoroughly explained in Tiberti et al. (2005). The geometry
265 and density of the shallow bodies, whose gravity effect was removed during the stripping-off

266 procedure, are known from about 60 logs of hydrocarbon wells drilled in the central Apennines, and
267 from several previously published studies on the subsurface geology of this region (e.g., Bally et al.,
268 1988; Anelli et al., 1994; Butler et al., 2004). In particular, density data used in this paper are
269 mainly after Mostardini and Merlini (1986). These data were integrated with other published
270 information (Table DR1).

271 The Tyrrhenian and Adriatic domains are characterized by gravity highs, whereas a relative
272 gravity low occurs in the axial sector of the Apennine fold-thrust belt (Fig. 4B). The gravity low is
273 ascribed to the regional deepening of both the Moho and the top of the crystalline basement (Tiberti
274 and Orlando, 2006).

275 In the Olevano-Antrodoco and Simbruini thrust areas (Fig. 1C), a second-order gravity low
276 affects the Bouguer and regional gravity anomalies (Figs. 3D, 4A, and 4B). This second-order
277 gravity low consists of a negative variation of about 10 mGal (Fig. 3D) and suggests the presence of
278 a relatively low density body in the middle crust. Provided that the effects of all the shallower
279 bodies have been properly removed, the 40 km wavelength of the 10-mGal-gravity-low is consistent
280 with a source depth between about 10 and 20 km since, at greater depth, density contrast of about \pm
281 100 kg/m^3 would affect an area broader than 40 km.

282 To define the areal extent of the 10-mGal-gravity low in the Olevano-Antrodoco and Simbruini
283 thrusts area, the tips (i.e., the lateral closures) of the second-order gravity low were searched in 70
284 gravity cross-sections arranged on a grid covering the study area, including the Olevano-Antrodoco
285 and the Simbruini thrust sheets (Fig. 1C). One of these cross-sections (i.e., the one coincident with
286 the CROP-11 profile) is shown in Fig. 3(D). The obtained tips were then plotted on the map of Fig.
287 5 and joined with a closed line (i.e., the dashed line encompassing the shaded area in Fig. 5). The
288 resulting area is roughly elliptical and N-S-elongated, being about 50 km long by 30 km wide. Its
289 N-S-trending long axis approximately coincides with the surface trace of the Olevano-Antrodoco
290 thrust.

291 Assuming that the second-order gravity low imaged in the gravity cross-section (Fig. 3D) and in
292 the maps of the Bouguer and regional gravity anomalies (Figs. 4A and 4B) is related to the
293 anticlinorium (Fig. 3B), we applied again the stripping-off procedure, which consisted, this time, of
294 calculating and removing from the Bouguer anomaly map (Fig. 4A) the effect of a geological body
295 with the same geometric and geologic characteristics (i.e., location, depth, and shape) of the
296 anticlinorium. The areal extent of the structure was approximately as inferred from the seismic
297 section (Fig. 3B) and from the anomalous shape of the gravity isolines (see inset in Fig. 4B), the
298 maximum overall thickness of the whole structure was fixed at about 8 km from the seismic profile
299 (Fig. 3B), dropping progressively toward the lateral closures of the structure as drawn in Fig. 3(B).
300 By a trial-and-error procedure, we found that the second-order gravity low could be best
301 compensated by assigning a density of 2570 kg/m^3 to the rocks forming the anticlinorium. Such a
302 density, for rocks lying at the depth of the mid-crustal anticlinorium, is consistent, for instance, with
303 low grade metamorphic rocks such as argillites or some kinds of phyllites. The occurrence of fluids
304 within these rocks may have reduced their density and increased their seismic reflectivity. The
305 reliability of the data used to model the anticlinorium is shown by the result of the stripping-off
306 procedure displayed in Fig. 4(C), where the second-order gravity low is almost completely absent
307 (i.e., compare insets in Figs. 4A, 4B, and 4C) and the main gravity anomalies become
308 approximately linear and aligned with the NW-SE regional structural trend.

309

310

311 **DISCUSSION**

312 The rotational origin of the Olevano-Antrodoco thrust is demonstrated by a positive orocline
313 test and by paleomagnetic data (Fig. 1B), which show a clockwise rotation of about 16° between
314 early-middle Miocene and middle Pliocene times (Sagnotti et al., 1994; Mattei et al., 1995, 1998;
315 Speranza et al., 1997). Paleomagnetic measurements are from seven sites on the Prenestini Mts,
316 which form the hangingwall of the Olevano-Antrodoco thrust. We think that more paleomagnetic

317 data are necessary to better constrain the rotation of the Olevano-Antrodoco thrust sheet and reduce
318 the error connected with past measurements (Mattei et al., 1995).

319 The analysis of the CROP-11 seismic image (Fig. 3A) shows the presence of a thick dome-
320 structure related to folding in the middle crust (i.e., the mid-crustal anticlinorium) right beneath the
321 Olevano-Antrodoco thrust (Fig. 3B). For the part visible in the CROP-11 profile, the Olevano-
322 Antrodoco thrust is imaged as a shallow thin-skinned thrust sheet, whose basal thrust emerges
323 above the crest region of the anticlinorium (Figs. 3C and 5). Due to the lack of appropriate
324 subsurface data, the subsurface geometry of the Olevano-Antrodoco thrust was mostly unknown
325 before the acquisition of the CROP-11 profile. We were able to compensate for the gravity
326 anomalies observed in both cross-section (Fig. 3D) and map (Fig. 4) views with a geological body
327 similar to that observed in the CROP-11 profile at the mid-crustal level and characterized by a
328 horizontal dimensions of about 50 by 30 km. The long axis of this structure is approximately N-S-
329 trending (Fig. 5). By combining these results with the seismic reflection image, we interpret the
330 near-elliptical geological body detected by the gravity analysis as a N-trending anticlinorium related
331 to contractional displacement on an basal shear zone lying at a middle-lower crust level (Figs. 3 and
332 5).

333 The timing of the anticlinorium development can be inferred, at least in part, by analyzing the
334 geometric relationship between the anticlinorium and the exposed or shallow thrusts, whose age is
335 known from previous studies (Fig. 2). In particular, in the CROP-11 image (Fig. 3B), the
336 Vallelonga thrust sheet is parallel to the forelimb of the underlying anticlinorium. This relationship
337 suggests that the Vallelonga thrust, whose age is late Messinian-very early Pliocene (i.e., see the
338 age of the Marsica thrust in Fig. 2), was involved in the growth of the anticlinorium. It follows that
339 the age of the anticlinorium should be early Pliocene (Fig. 2). In middle Pliocene time, contractional
340 deformation was mostly inactive across the presently-exposed portion of the central Apennines, and
341 normal faulting was already active at least in the inner and axial sectors of the belt (Fig. 2).
342 Furthermore, the geometric relationship between the Olevano-Antrodoco thrust and the

343 anticlinorium (Fig. 3B) is consistent with the inferred age of anticlinorium growth (i.e., early
344 Pliocene time). The Olevano-Antrodoco thrust, in fact, whose age is late Messinian-early Pliocene
345 (Fig. 2), seems partly involved in the mid-crustal folding. The hypothesized tectonic interaction
346 between the Olevano-Antrodoco thrust and the underlying anticlinorium likely took place during
347 the latest phase of thrust activity (i.e., during early Pliocene time).

348 To verify whether the Olevano-Antrodoco thrust is folded, we analyzed the elevation pattern of
349 the emerging thrust (A-B and C-D cross-sections in Fig. 6B). The longitudinal topographic profile
350 of the Olevano-Antrodoco thrust has a gentle antiformal shape with elevation varying between
351 about 700 m and 1600 m above sea level. The minimum elevation of the Olevano-Antrodoco thrust
352 is not known because, toward the south, this structure is covered by recent volcanic deposits (Fig.
353 6A). The antiformal longitudinal profile of the Olevano-Antrodoco thrust (Fig. 6B) suggests that the
354 thrust is folded. This inference is true, however, only if the profile (Fig. 6B) actually tracks the
355 same structural depth along the thrust surface; otherwise, the antiformal shape may be connected
356 with a variation of structural depth along the thrust. The amplitude of the antiformal shape (Fig. 6B)
357 suggests, however, that such geometry is more an expression of a regional folding than an apparent
358 structure due to the intersection between the profile and the thrust. If this inference is true, then the
359 longitudinal folding of the Olevano-Antrodoco thrust is consistent with the hypothesis that the mid-
360 crustal anticlinorium produced a surface uplift.

361 Further evidence indicating possible surface uplift in the study area may come from
362 sedimentologic studies. On top of the Simbruini Mountains (Fig. 6A), several conglomeratic
363 deposits are exposed at different altitudes (Accordi and Carbone, 1986). Most of these deposits are
364 still to be studied, mapped, and dated in detail. In some of these conglomerates, clasts deriving from
365 lower Cretaceous platform carbonates have been found (M. Parotto, personal communication). This
366 observation may imply the erosion of at least 1000 m of a Cretaceous-Paleogene carbonate
367 succession (Accordi and Carbone, 1986); however, the occurrence of hiatuses in the Mesozoic-
368 Paleogene carbonate succession of central Italy makes this evidence not sufficient to demonstrate

369 the erosion during Pliocene time. Moreover, in the Simbruini-Roveto area, the Puddinghe di
370 Canistro e Broccostella Formation (indicated as main Pliocene conglomerates in Fig. 6A) consists
371 of lower Pliocene conglomerates including rounded, exotic, sedimentary clasts, which are probably
372 derived from hinterland areas located toward the west and northwest (Cipollari and Cosentino,
373 2002). These conglomerates unconformably rest on Mesozoic carbonates or synorogenic flysch
374 deposits (Accordi and Carbone, 1986). The presence of lower Pliocene conglomeratic deposits in
375 the Simbruini-Roveto area (Fig. 6A) suggests the occurrence of significant erosion in the area
376 located to the west and northwest of these deposits (Fig. 5), such erosion being possibly connected
377 with the hypothesized surface uplift generated by anticlinorium growth during early Pliocene time.

378 Based on the above evidence and inferences, we propose the following model for orogenic
379 curvature of the southern portion of the Umbrian Arc (Fig. 7). The Olevano-Antrodoco thrust
380 developed and propagated during late Messinian-early Pliocene time with an eastward vergence.
381 The thrust underwent an orogenic clockwise curvature when it ran into the surface uplift induced by
382 the growing mid-crustal anticlinorium, which then raised and folded the Olevano-Antrodoco thrust.
383 This process halted the eastward advancement of the Olevano-Antrodoco thrust. The interaction
384 between the Olevano-Antrodoco thrust and the anticlinorium-related surface uplift caused
385 nonplane-strain deformation recorded by vertical-axis rotations detected in the hangingwall of the
386 Olevano-Antrodoco thrust, and by right-lateral displacements detected on the thrust surface
387 (Castellarin et al., 1978; Salvini and Vittori, 1982; Mattei et al., 1995). According to this model, the
388 southern portion of the Umbrian Arc can be classified as a progressive arc (Weil and Sussman,
389 2004), where the orogenic curvature was progressively acquired during the propagation of the thrust
390 in late Messinian-early Pliocene time. The three-dimensional architecture of the anticlinorium and
391 its relationships with the adjacent structures are mostly inferred from two-dimensional evidence
392 (Fig. 3). Uncertainty and error inherent with modeling a three-dimensional structure from two-
393 dimensional evidence compel a revision of this model in the future when new subsurface data will
394 be available.

395 The model proposed in this paper for the curvature of the southern sector of the Umbrian Arc
396 agrees with several previous models in that the main cause of curvature is a geologic obstacle that
397 obstructed thrust migration (e.g., Eldredge et al., 1985; Calamita and Deiana, 1988). In previous
398 studies, the impingement of the Olevano-Antrodoco thrust was mostly ascribed to the stiff
399 carbonate succession forming the Adriatic-Apulian foreland and the thrust sheets of the central
400 Apennines (Ghisetti and Vezzani, 1997). In contrast, we propose that the impingement of the
401 Olevano-Antrodoco thrust was caused by a mid-crustal anticlinorium, which was first imaged in the
402 CROP-11 profile (Billi et al., 2006). For some aspects, this latter model refines the one proposed by
403 Lavecchia et al. (1988), who hypothesized the role of deep-crust structures on the formation of the
404 Umbrian Arc, but could not ascertain the occurrence of these structures because of the lack of
405 proper subsurface data.

406 For several geometric and kinematic characteristics, the mid-crustal anticlinorium imaged in the
407 CROP-11 profile (Fig. 3B) is similar to some mid-crustal basement thrusts depicted in the Andean
408 backthrust belt, Bolivia, by McQuarrie and DeCelles (2001) and in other fold-thrust belts (e.g.,
409 Alps, Appalachians, Caledonides, Himalaya, and Sevier belt; see Hatcher and Hooper, 1992;
410 Yonkee, 1992; DeCelles et al., 1995; Kley, 1996; McBride and England 1999; Wobus et al., 2005).
411 The frequency, in fold-thrust belts, of curved thrusts and mid-crustal thick folds such as that
412 depicted in this paper suggests that mid-crustal contractional structures may be revealed as one of
413 the important factors controlling local or regional curvature in orogens. The mature and final
414 evolutionary phases of fold-thrust belts, in fact, are often characterized by both deep folds, and
415 inner shallow out-of-sequence thrusts (e.g., Wobus et al., 2005), which both contribute to re-
416 establishing orogenic taper subcriticality. As such, deep folds may be at the origin of topographic
417 obstacles that obstruct the propagation of inner shallow thrusts such as the Olevano-Antrodoco
418 thrust in the central Apennines.

419

420

421 **CONCLUSIONS**

422 (1) Results from the analysis of geological and geophysical data from the central Apennines are
423 consistent with a causal link between clockwise rotation of the southern limb of the Umbrian
424 Arc during late Neogene time and the penecontemporaneous growth of a thick mid-crustal
425 anticlinorium. More evidence is required to fully support our hypothesis. In particular, more
426 subsurface data are necessary to define the three-dimensional structure of the anticlinorium, and
427 additional paleomagnetic evidence is necessary to better constrain the rotation of the southern
428 limb of the Umbrian Arc.

429 (2) The tectonic process invoked to explain rotation of the southern limb of the Umbrian Arc (i.e.,
430 by developing a mid-crustal anticlinorium whose surface effects obstructed the advancement of
431 an inner out-of-sequence shallow thrust) is a novel explanation for the origin of orogenic arcs
432 around the world (e.g., Macedo and Marshak, 1999; Schellart and Lister, 2004; Sussman and
433 Weil, 2004); however, because both out-of-sequence shallow thrusts and mid-crustal thick folds
434 are common in curved fold-thrust belts, mid-crustal contractional structures may be the cause of
435 thrust curvatures at the local or regional scale in other orogenic systems.

436 (3) Results from this study show that the solution of complex geological issues, such as the
437 comprehension of orogenic arcs, requires the contribution of appropriate subsurface data and
438 their integration into a multidisciplinary research including, for instance, geomorphologic,
439 geophysical, stratigraphic, and tectonic analyses. In this study, results from subsurface
440 prospecting by seismic and gravity methods and their integration in a multidisciplinary research
441 compelled the revision of previous models of arc development and thrust evolution in the
442 central Apennines, the past models being based mainly on surface data.

443

444 **Acknowledgments:** We thank G. Cavinato, D. Cosentino, J. Keller, C. Kluth, L. Orlando, M.
445 Parotto, F. Storti and all colleagues who have worked with us at the CROP-11 Project. Suggestions
446 from P. Cipollari and D. Cosentino about the timing of thrusts in the central Apennines, and from J.

447 Bausà-Llecha and S. Tavani about thrust tectonics were very important to improve the paper.
448 Discussions with R. Basili were very helpful. We thank M. Barchi, G. Gutierrez-Alonso, S.
449 Johnston, K. Karlstrom, M. Mattei, S. Mazzoli, B. Murphy, and A. Weil for their constructive and
450 careful revisions, which greatly improved the paper.
451

452 **REFERENCES CITED**

- 453 Accordi, G., and Carbone, F., eds., 1986, Lithofacies map of Latium-Abruzzi and neighbouring areas, scale
454 1:250,000, 1 sheet, Rome, Consiglio Nazionale delle Ricerche.
- 455 Anelli, L., Gorza, M., Pieri, M., and Riva, M., 1994, Subsurface well data in the Northern Apennines:
456 Memorie della Società Geologica Italiana, v. 48, p. 461-471.
- 457 Bally, A. W., Burbi, L., Cooper, C., and Ghelardoni, R., 1988, Balanced sections and seismic reflection
458 profiles across the central Apennines: Memorie della Società Geologica Italiana, v. 35, p. 257-310.
- 459 Barchi, M., Minelli, G., and Piali, G., 1998, The CROP 03 profile: a synthesis of results on deep structures of
460 the Northern Apennines: Memorie della Società Geologica Italiana, v. 52, p. 383-400.
- 461 Billi, A., Tiberti, M. M., Cavinato, G. P., Cosentino, D., Di Luzio, E., Keller, J. V. A., Kluth, C., Orlando, L.,
462 Parotto, M., Praturlon, A., Romanelli, M., Storti, F., and Wardell, N., 2006, First results from the CROP-
463 11 deep seismic profile, central Apennines, Italy: evidence of mid-crustal folding: Journal of the
464 Geological Society, London, v. 163, p. 583-586.
- 465 Calamita, F., and Deiana, G., 1988, The arcuate shape of the Umbria-Marche-Sabina Apennines (central
466 Italy): Tectonophysics, v. 146, p. 139-147.
- 467 Carozzo, M. T., Luzio, D., Margiotta, C., and Quarta, T., 1991, Gravity map of Italy, scale 1:500,000, 3
468 sheets, Florence, Italy, SELCA.
- 469 Cassinis, R., Scarascia, S., and Lozej, A., 2003, The deep crustal structure of Italy and surrounding areas from
470 seismic refraction data. A new synthesis: Bollettino della Società Geologica Italiana, v. 122, p. 365-376.
- 471 Castellarin, A., Colacicchi, R., and Praturlon, A., 1978, Fasi distensive, trascorrenze e sovrascorrimenti lungo
472 la "Linea Ancona-Anzio", dal Lias medio al Pliocene: Geologica Romana, v. 17, p. 161-189.
- 473 Cavinato, G., and DeCelles, P. G., 1999, Extensional basins in tectonically bimodal central Apennines fold-
474 thrust belt, Italy: response to corner flow above a subducting slab in retrograde motion: Geology, v. 27, p.
475 955-958.
- 476 Cavinato, G. P., Carusi, C., Dall'Asta, M., Miccadei, E., and Piacentini, T., 2002, Sedimentary and tectonic
477 evolution of Plio-Pleistocene alluvial and lacustrine deposits of Fucino Basin (central Italy): Sedimentary
478 Geology, v. 148, p. 29-59.
- 479 Channel, J. E. T., Lowrie, W., Medizza, F., and Alvarez, W., 1978. Paleomagnetism and tectonics in Umbria,
480 Italy. Earth and Planetary Science Letters, v. 39, p. 199-210.
- 481 Cipollari, P., 1995, Modalità e tempi di propagazione del sistema catena-avanfossa-nella zona di incontro tra
482 Appennino settentrionale e Appennino centrale [Ph.D. thesis]: Rome, Italy, Università "La Sapienza",
483 229 p.
- 484 Cipollari, P., and Cosentino, D., 1992, La linea Olevano-Antrodoco: contributo della biostratigrafia alla sua
485 caratterizzazione cinematica: Studi Geologici Camerti, v. 1991/2, 143-149.
- 486 Cipollari, P., and Cosentino, D., 1995, Miocene unconformities in the central Apennines: geodynamic
487 significance and sedimentary basin evolution: Tectonophysics, v. 252, p. 375-389.

488 Cipollari, P., and Cosentino, D., 2002, Convegno-escursione COFIN'99: Evoluzione cinematica del sistema
489 orogenico dell'Appennino centro-meridionale: caratterizzazione stratigrafico-strutturale dei bacini
490 sintettonici: Università Roma Tre, Rome, Italy, p. 1-84.

491 Cipollari, P., Cosentino, D., and Perilli, N., 1993, Analisi biostratigrafica dei depositi terrigeni a ridosso della
492 Linea Olevano-Antrodoco: *Geologica Romana*, v. 29, p. 495-513.

493 Corrado, S., 1995, Nuovi vincoli geometrico-cinematici all'evoluzione neogenica del tratto meridionale della
494 linea Olevano-Antrodoco: *Bollettino della Società Geologica Italiana*, v. 114, p. 245-276.

495 Cosentino, D., Cipollari, P., and Pipponzi, G., 2003, Il sistema orogenico dell'Appennino centrale: vincoli
496 stratigrafici e cronologia della migrazione: *Studi Geologici Camerti*, v. 2003/1, p. 85-99.

497 Coward, M. P., De Donatis, M., Mazzoli, S., Paltrinieri, W., and Wezel, F. C., 1999, Frontal part of the
498 Northern Apennines fold and thrust belt in the Romagna-Marche area (Italy): shallow and deep structural
499 styles: *Tectonics*, v. 18, p. 559-574.

500 Davis, G. H., Reynolds, S.J., 1996, *Structural Geology of Rocks and Regions*: New York, John Wiley, pp.
501 776.

502 DeCelles, P. G., Lawton, T. F., and Mitra, G., 1995, Thrust timing, growth of structural culminations, and
503 synorogenic sedimentation in the type Sevier orogenic belt, Western United States: *Geology*, v. 23, p.
504 699-702.

505 Dewey, J. F., Helman, M. L., Turco, E., Hutton, D. H. W., and Knott, S. D., 1989, Kinematics of the western
506 Mediterranean, *in* Coward, M. P., Dietrich, D., and Park, R. G., eds., *Alpine Tectonics*, Geological
507 Society Special Publication, v. 45, p. 265-283.

508 Di Luzio, E., Mele, G., Tiberti, M. M., Cavinato, G. P., and Parotto, M., 2008, Moho deepening and shallow
509 upper crustal delamination beneath the central Apennines: *Earth Planet. Sci. Lett.*, in press,
510 doi:10.1016/j.epsl.2008.09.018.

511 Eldredge, S., Bachtadse, V., and Van der Wou, R., 1985, Paleomagnetism and the orocline hypothesis:
512 *Tectonophysics*, v. 119, p. 153-179.

513 Faccenna, C., Piromallo, C., Crespo-Blanc, A., and Jolivet, L., 2004, Lateral slab deformation and the origin
514 of the western Mediterranean arcs: *Tectonics*, v. 23, TC1012, doi:10.1029/2002TC001488.

515 Ghisetti, F., and Vezzani, L., 1997, Interfering paths of deformation and development of arcs in the fold-and-
516 thrust belt of the central Apennines: *Tectonics*, v. 16, p. 523-536.

517 Ghisetti, F., Barchi, M., Bally, A. W., Moretti, I., and Vezzani, L., 1993, Conflicting balanced structural
518 sections across the Central Apennines (Italy): problems and implications, *in* Spencer, A. M., ed.,
519 *Generation, Accumulation and Production of Europe's Hydrocarbons: Special Publication of the*
520 *European Association of Petroleum Geoscientists*, v. 3, p. 219-231.

521 Hammer, S., 1963, Deep gravity interpretation by stripping: *Geophysics*, v. 28, p. 369-378.

522 Hatcher, R. D., and Hooper, R. J., 1992, Evolution of crystalline thrust sheet in the internal parts of mountain
523 chains, *in* McClay, K. R., ed., *Thrust Tectonics*, New York, Chapman & Hall, p. 217-233.

524 Hirt, A., and Lowrie, W., 1988, Paleomagnetism of the Umbria-Marches orogenic belt: *Tectonophysics*, v.
525 146, p. 91-103.

526 Jolivet, L., Faccenna, C., Goffé, B., Mattei, M., Rossetti, F., Brunet, C., Storti, F., Funicello, R., Cadet, J. P.,
527 D'Agostino, N., and Parra, T., 1998, Midcrustal shear zones in postorogenic extension: Example from the
528 northern Tyrrhenian Sea: *Journal of Geophysical Research*, v. 103, p. 12,123-12,160.

529 Kley, J., 1996, Transition from basement involved to thin-skinned thrusting in the Cordillera Oriental of
530 southern Bolivia: *Tectonics*, v. 15, p. 763-775.

531 Lavecchia, G., Minelli, G., and Piali, G., 1988, The Umbria-marche arcuate fold belt: *Tectonophysics*, v.
532 146, p. 125-137.

533 Macedo, J., and Marshak, S., 1999, Controls on the geometry of fold-thrust belt salients: *Geological Society
534 of America Bulletin*, v. 111, p. 1808-1822.

535 Malinverno, A., and Ryan, W. B. F., 1986, Extension in the Tyrrhenian Sea and shortening in the Apennines
536 as result of arc migration driven by sinking of the lithosphere: *Tectonics*, v. 5, p. 227-254.

537 Marshak, S., 2004, Salients, recesses, arcs, oroclines, and syntaxes-A review of ideas concerning the
538 formation of map-view curves in fold-thrust belts, *in* McClay, K. R., ed., *Thrust Tectonics and
539 Hydrocarbon Systems: AAPG Memoir*, v. 82, p. 131-156.

540 Mattei, M., Funicello, R., and Kissel, C., 1995, Paleomagnetic and structural evidence for Neogene block
541 rotations in the Central Apennines, Italy: *Journal of Geophysical Research*, v. 100, p. 17,863-17,883.

542 Mattei, M., Speranza, F., Sagnotti, L., Funicello, R., and Faccenna, C., 1998, Paleomagnetic constraints to
543 the tectonic evolution of the northern Italian Peninsula: *Memorie della Società Geologica Italiana*, v. 52,
544 p. 469-478.

545 Mazzoli, S., Corrado, S., De Donatis, M., Scrocca, D., Butler, R. W. H., Di Bucci, D., Naso, G., Nicolai, C.,
546 and Zucconi, V., 2000, Time and space variability of “thin-skinned” and “thick-skinned” thrust tectonics
547 in the Apennines (Italy): *Rendiconti Lincei, Scienze Fisiche e Naturali*, v. 11, p. 5-39.

548 Mazzoli, S., D'Errico, M., Aldega, L., Corrado, S., Invernizzi, C., Shiner, P., and Zattin, M., 2008, Tectonic
549 burial and “young” (<10 Ma) exhumation in the southern Apennines fold-and-thrust belt (Italy): *Geology*,
550 v. 36, p. 243-246.

551 McBride, J. H., and England, R. W., 1999, Window into the Caledonian orogen: structure of the crust beneath
552 the East Shetland platform, United Kingdom: *Geological Society of America Bulletin*, v. 111, p. 1030-
553 1041.

554 McQuarrie, N., and DeCelles, P., 2001, Geometry and structural evolution of the central Andean backthrust
555 belt, Bolivia: *Tectonics*, v. 20, p. 669-692.

556 Mele, G., Sandvol, E., and Cavinato, G.P., 2006, Evidence of crustal thickening beneath the central
557 Apennines (Italy) from teleseismic receiver functions: *Earth and Planetary Science Letters*, v. 249, p. 425-
558 435.

559 Mostardini, F., and Merlini, S., 1986, Appennino centro-meridionale. Sezioni geologiche e proposta di
560 modello strutturale: *Memorie della Società Geologica Italiana*, v. 35, p. 177-202.

561 Muttoni, G., Argnani, A., Kent, D. V., Abrahamsen, N., and Cibin, U., 1998, Paleomagnetic evidence for
562 Neogene tectonic rotations in the northern Apennines, Italy: *Earth and Planetary Science Letters*, v. 154,
563 p. 25-40

564 Park, J.-O., Tetsuro, T., Shuichi, K., Narumi, T., Ayako, N., Seiichi, M., Yoshiyuki, K., and Yoshiteru, K.,
565 2000, Out-of-sequence thrust faults developed in the coseismic slip zone of the 1946 Nankai earthquake
566 (Mw=8.2) off Shikoku, southwest Japan: *Geophysical Research Letters*, v. 27, p. 1033-1036.

567 Parotto, M., and Praturlon, A., 1975, Geological summary of central Apennines: *Quaderni de La Ricerca*
568 *Scientifica*, v. 90, p. 257-311.

569 Patacca, E., and Scandone, P., 2001, Late thrust propagation and sedimentary response in the thrust-belt-
570 foredeep system of the southern Apennines (Pliocene-Pleistocene), *in* Vai, G. B., and Martini, I. P. eds.,
571 *Anatomy of an Orogen: the Apennines and Adjacent Mediterranean Basins*, Kluwer Academic Publishers,
572 London, p. 401-440.

573 Patacca, E., Sartori, R., and Scandone, P., 1992, Tyrrhenian basin and Apenninic arcs: kinematic relations
574 since late Tortonian times: *Memorie della Società Geologica Italiana*, v. 45, p. 425-451.

575 Patacca E., Scandone, P., Di Luzio, E., Cavinato, G. P., and Parotto, M., 2008, Structural architecture of the
576 central Apennines: Interpretation of the CROP 11 seismic profile from the Adriatic coast to the
577 orographic divide: *Tectonics*, v. 27, TC3006, doi:10.1029/2005TC001917.

578 Rosenbaum, G., and Lister, G. S., 2004, Formation of arcuate orogenic belts in the western Mediterranean
579 region, *in* Sussman, A. J., and Weil, A. B., eds., *Orogenic Curvature: Integrating Paleomagnetic and*
580 *Structural Analyses: Geological Society of America Special Paper 383*, p. 41-56.

581 Royden, L., Patacca, E., and Scandone, P., 1987, Segmentation and configuration of subducted lithosphere in
582 Italy: an important control on thrust-belt and foredeep-basin evolution: *Geology*, v. 15, p. 714-717.

583 Sagnotti, L., Mattei, M., Faccenna, C., and Funiciello, R., 1994, Paleomagnetic evidence for no tectonic
584 rotation of the central Italy margin since upper Pliocene: *Geophysical Research Letters*, v. 21, p. 481-484.

585 Salvini, F., and Vittori, E., 1982, Analisi strutturale della linea Olevano-Antrodoco-Posta (Ancona-Anzio
586 Auct.): metodologia di studio delle deformazioni fragili e presentazione del tratto meridionale: *Memorie*
587 *della Società Geologica Italiana*, v. 24, p. 337-356.

588 Satolli S., Speranza, F., and Calamita, F., 2005, Paleomagnetism of the Gran Sasso range salient (central
589 Apennines, Italy): pattern of orogenic rotations due to translation of a massive carbonate indenter:
590 *Tectonics*, v. 24, TC4019, doi:10.1029/2004TC001771.

591 Schellart, W. P., and Lister, G. S., 2004, Tectonic models for the formation of arc-shaped convergent zones
592 and backarc basins, *in* Sussman, A. J., and Weil, A. B., eds., *Orogenic Curvature: Integrating*
593 *Paleomagnetic and Structural Analyses: Geological Society of America Special Paper 383*, p. 237-258.

594 Servizio Geologico d'Italia, 1967, Carta Geologica d'Italia alla scala 1:100,000, Foglio "Sora", scale
595 1:100,000, 1 sheet, Florence, Italy, Litografia Artistica Cartografica.

596 Speranza, F., Sagnotti, L., and Mattei, M., 1997, Tectonics of the Umbria-Marche-Romagna Arc (central
597 northern Apennines, Italy): New paleomagnetic constraints: *Journal of Geophysical Research*, v. 102, p.
598 3153-3166.

599 Steckler, M. S., Piana Agostinetti, N., Wilson, C. K., Roselli, P., Seeber, L., Amato, A., and Lerner-Lam, A.,
600 2008, Crustal structure in the Southern Apennines from teleseismic receiver functions: *Geology*, v. 36, p.
601 155-158.

602 Sussman, A. J., and Weil, A. B., eds., 2004, *Orogenic Curvature: Integrating Paleomagnetic and Structural*
603 *Analyses: Geological Society of America Special Paper 383.*

604 Sussman, A. J., Butler, R. F., Dinares-Turell, J., and Verges, J., 2004, vertical axis rotation of a foreland fold:
605 an example from the southern Pyrenees: *Earth and Planetary Science Letters*, v. 218, p. 435-449.

606 Tiberti, M. M., and Orlando, L., 2006, 2D gravity modelling along the CROP11 seismic profile: *Bollettino di*
607 *Geofisica Teorica ed Applicata*, v. 47, p. 447-454.

608 Tiberti, M. M., Orlando, L., Di Bucci, D., Bernabini, M., and Parotto, M., 2005, Regional gravity anomaly
609 map and crustal model of the Central-Southern Apennines (Italy): *Journal of Geodynamics*, v. 40, p. 73-
610 91.

611 Vezzani, L., and Ghisetti, F., 1993, *Carta geologica dell'Abruzzo*, scale 1:100,000, 1 sheet, Florence, Italy,
612 SELCA.

613 Weil, A. B., 2006, Kinematics of orocline tightening in the core of an arc: Paleomagnetic analysis of the
614 Ponga Unit, Cantabrian Arc, northern Spain: *Tectonics*, v. 25, TC3012, doi:10.1029/2005TC001861.

615 Weil, A. B., and Sussman, A. J., 2004, Classifying curved orogens based on timing relationships between
616 structural development and vertical-axis rotations, implications, *in* Sussman, A. J., and Weil, A. B., eds.,
617 *Orogenic Curvature: Integrating Paleomagnetic and Structural Analyses: Geological Society of America*
618 *Special Paper 383*, p. 1-15.

619 Wobus, C., Heimsath, A., Whipple, K., and Hodges, K., 2005, Active out-of-sequence thrust faulting in the
620 central Nepalese Himalaya: *Nature*, v. 434, p. 1008-1011.

621 Yonkee, W. A., 1992, Basement-cover relations, Sevier orogenic belt, northern Utah: *Geological Society of*
622 *America Bulletin*, v. 104, p. 280-302.

623

624 **FIGURE CAPTIONS**

625 **Figure 1. (A)** Digital elevation model of Italy and surrounding areas. Main Cenozoic fold-thrust
626 belts are shown. The northern and southern arcs of the Apennine fold-thrust belt are indicated.
627 The main curved structure of the northern arc is the Umbrian Arc (Eldredge et al., 1985). The
628 study area is located in the central Apennines and includes the N-S-trending southern limb of
629 the Umbrian Arc, also known as the Olevano-Antrdoco thrust. **(B)** Geological map of the
630 northern Apennines. The Cervarola flysch mainly consists of sandstones and shales. Epi-
631 Ligurian units are mainly sandstones and marls derived from a pristine, continent-ocean margin.
632 Ligurian units are ophiolites and sedimentary and low-grade metamorphic rocks derived from a
633 pristine, oceanic basin. The Sabina carbonaceous sequence include transitional carbonates
634 originally located between the Latium platform carbonates (central Italy) and the Umbrian
635 pelagian carbonates (northern Apennines). The Sabina sequence includes also a thick sequence
636 of platform limestones (Calcare Massiccio Formation) at the base of the succession. The Latium
637 carbonates are mostly platform limestones and dolostones. The Tuscan succession consists of a
638 pile of carbonates, marls, shales, evaporites, and sandstones deposited in different environments
639 succeeded through Mesozoic-Paleogene times. **(C)** Geological map of the central Apennines.
640 “th.” stands for thrust sheet. Arrows are tilt corrected paleomagnetic declinations (Mattei et al.,
641 1998).The CROP-11 seismic profile (“W-E”) cuts across the southern limb (i.e., the Olevano-
642 Antrodoco thrust) of the Umbrian Arc.

643

644 **Figure 2.** Time-distance diagram including thrusting, out-of-sequence thrusting, and post-orogenic
645 basin sedimentation in the central Apennines (modified after Cavinato and DeCelles, 1999). The
646 diagram refers to a SW-NE transect across the central Apennines including all main thrusts and
647 extensional basins. The diagram shows that the central Apennines mainly evolved by in-
648 sequence thrusting. Some late out-of-sequence thrusts also occurred. In each locality, the onset
649 of extensional basin sedimentation is the temporal upper limit for contractional tectonics. The
650 inferred age for the mid-crustal anticlinorium (Fig. 3B) is also shown.

651

652 **Figure 3. (A)** Central segment of the CROP-11 seismic reflection profile. See the related track
653 (“W-E”) in Fig. 1(C). TWTT is two ways travel time. The entire CROP-11 profile from the
654 Tyrrhenian Sea to the Adriatic Sea and the related acquisition and processing parameters are
655 available in Billi et al. (2006). **(B)** Line drawing and interpretation of the CROP-11 profile
656 displayed in (A). The mid-crustal anticlinorium (i.e., indicated as “hangingwall”) involves

657 reflections between about 7-9 (i.e., the mid-crustal shear zone) and the topographic surface in
658 the footwall of the Olevano-Antrodoco thrust. **(C)** Enlargement (left) and related interpretation
659 (right) of the sector of the CROP-11 profile including the near-surface portion of the Olevano-
660 Antrodoco thrust, which is interpreted as a shallow, low-angle, reverse structure. **(D)** Gravity
661 cross-section along the segment of the CROP-11 profile shown in (A). The shaded area is the
662 effect (i.e., negative) induced by the tectonic duplication (i.e., the anticlinorium) shown in the
663 CROP-11 profile. Without this structure, the gravity cross-section would run along the upper
664 (dotted) line.

665

666 **Figure 4.** Gravity maps of central Italy. **(A)** Bouguer anomaly map. **(B)** Regional gravity map.
667 **(C)** Regional gravity map after the removal (stripping-off procedure) of the effect of the mid-
668 crustal anticlinorium shown in Fig. 3(B).

669

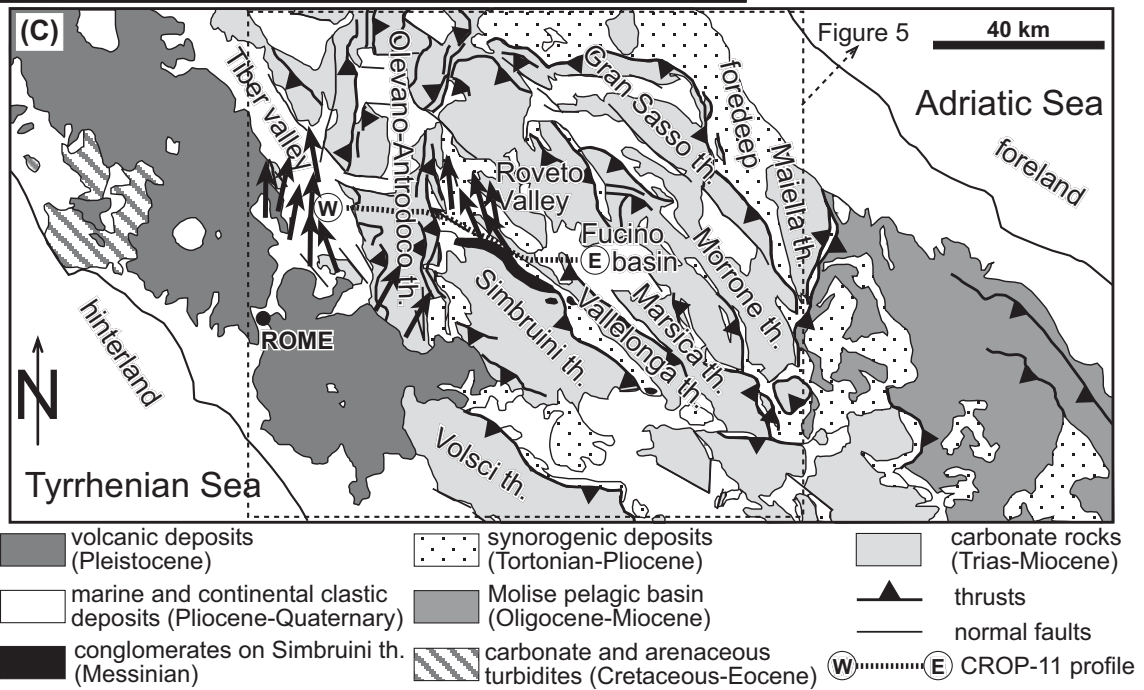
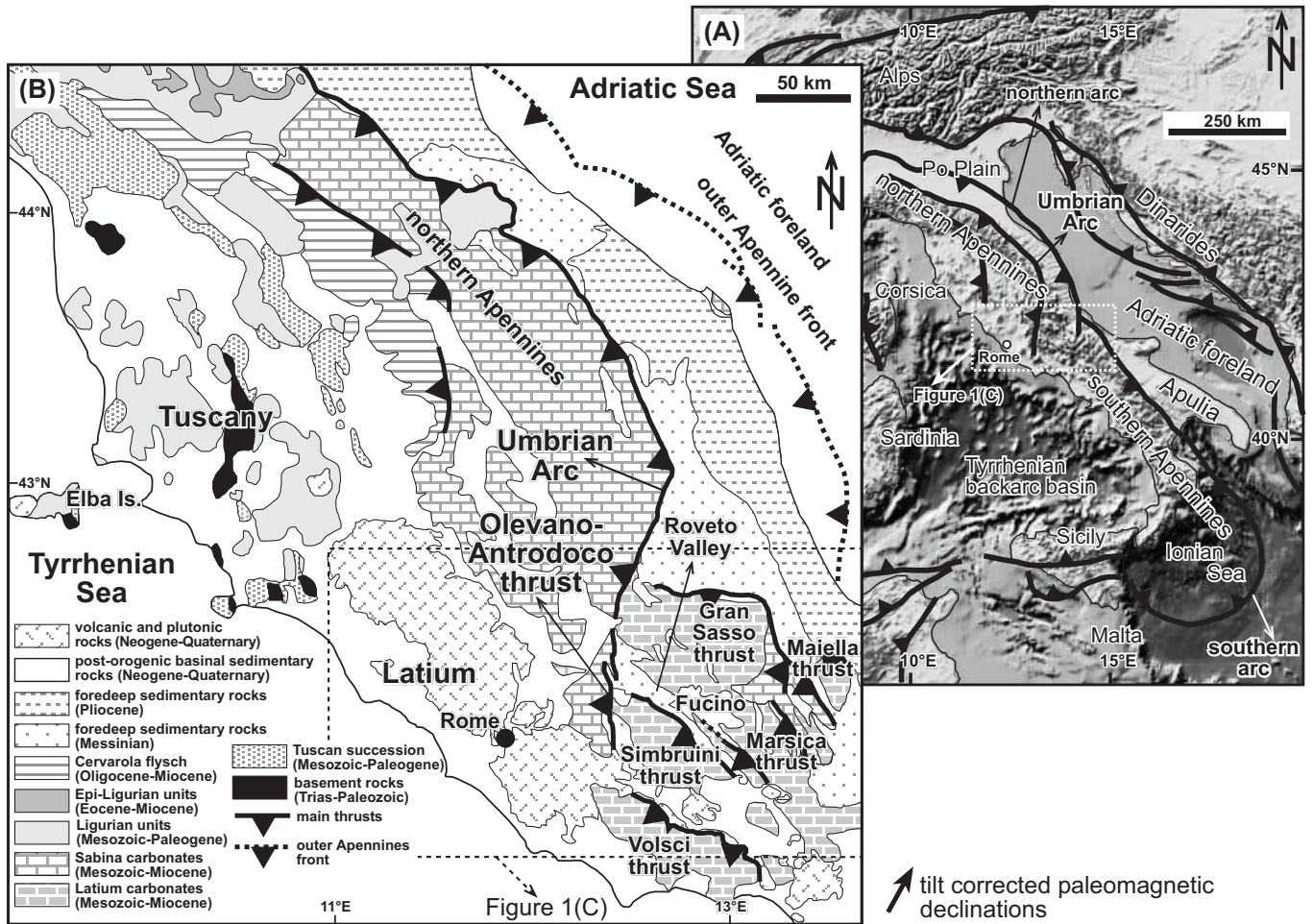
670 **Figure 5.** Schematic tectonic map of central Italy (location of this figure is indicated in Fig. 1C).
671 The shaded area represents the gravity anomaly induced by tectonic duplication associated with
672 the anticlinorium imaged in the CROP-11 profile (Fig. 3B). This area is interpreted to represent
673 a N-trending mid-crustal anticlinorium related to displacement on a basal shear zone lying at the
674 middle-lower crust level (Fig. 3B). The shaded area is drawn by joining the points representing
675 the projection on the map of the lateral tips of the gravity anomaly connected with the
676 anticlinorium and observed on 70 gravity cross-sections (see one of these cross-sections in Fig.
677 3D). As such, this area represents the approximate areal extent (i.e., where the gravity signature
678 induced by the tectonic duplication is sufficiently marked to be detected) of the mid-crustal
679 anticlinorium. The paleomagnetic data are from Sagnotti et al. (1994) and Mattei et al. (1995).

680

681 **Figure 6.** **(A)** Geological map of central Apennines. The tracks of topographic cross-sections
682 shown in (B) are displayed. The flysch deposits (i.e., mainly sandstones with shale
683 intercalations) are undifferentiated and indicated as Tortonian-Pliocene in age. Because of the
684 northeastward progression of the fold-thrust belt, flysch deposits are younger toward the
685 northeast. In the Roveto Valley, flysch deposits are Messinian in age and are overlain by the
686 Olevano-Antrodoco thrust, whose latest age is, therefore, post-Messinian (i.e., early Pliocene)
687 (Cipollari and Cosentino, 2002). **(B)** Projection of the altitude of the emergence of the Olevano-
688 Antrodoco thrust on the A-B and C-D tracks. The vertical scale is greatly exaggerated.

689

690 **Figure 7.** Schematic cross-sectional cartoon (see the approximate AA' track in Fig. 5) showing the
691 interaction between the development of the Olevano-Antrodoco thrust and that of the mid-
692 crustal anticlinorium during early Pliocene time. During this time, the Olevano-Antrodoco
693 thrust developed and migrated toward the east as a shallow out-of-sequence structure. In the
694 mean time, a mid-crustal thick anticlinorium developed ahead (east) of the Olevano-Antrodoco
695 thrust by folding a thick section of the middle-upper crust and by generating a surface uplift. As
696 the Olevano-Antrodoco thrust run into the anticlinorium, the thrust was raised and folded by the
697 growing anticlinorium and the thrust propagation was eventually halted. The northern
698 prolongation of the Olevano-Antrodoco thrust kept advancing toward the east, thus ultimately
699 forming the Umbrian Arc thanks to the impingement of the Olevano-Antrodoco thrust against
700 the mid-crustal anticlinorium. The fold is modified after Davis and Reynolds (1996).
701



↑ tilt corrected paleomagnetic declinations

